ELSEVIER

Journal of Alloys and Compounds 356–357 (2003) 639–643

Journal of ALLOYS AND COMPOUNDS

www.elsevier.com/locate/jallcom

Synthesis and hydrogen sorption properties of nanocrystalline $Mg_{1.9}M_{0.1}Ni$ (M=Ti, Zr, V) obtained by mechanical alloying

T. Spassov[a,b,*], P. Solsona[a], S. Bliznakov[c], S. Suriñach[a], M.D. Baró[a]

[a]*Departament de Física, Facultat de Ciencies, Universitat Autonoma de Barcelona, LMT, Edifici Cc, 08193 Bellaterra, Spain*
[b]*Department of Chemistry, University of Sofia 'St. Kl. Ohridski', 1 J. Bourchier Str., 1126 Sofia, Bulgaria*
[c]*Central Laboratory of Electrochemical Power Sources, Bulgarian Academy of Sciences, Sofia, Bulgaria*

Received 1 June 2002; accepted 1 September 2002

Abstract

Nanocrystalline and nano-/amorphous $Mg_{1.9}M_{0.1}Ni$ (M=Ti, Zr, V) alloys were synthesized by mechanical alloying (MA) as well as by MA followed by annealing. The ball milling and heat treatment conditions for obtaining amorphous or nanocrystalline alloys were optimised for different alloy compositions. The phase composition, microstructure and morphology of the as-milled and heat-treated powders were determined by XRD, TEM and SEM. Thermal stability, crystallization and grain growth processes in the nano-/amorphous alloys were investigated, too. After milling the alloys have hexagonal Mg_2Ni crystal structure. The crystallites size of the milled as well as of the milled and then annealed alloys was estimated to be in the range of 10–20 nm. The grain size increases slightly during heating to above 700 K. Hydrogen sorption kinetics and storage capacity of the as milled nano-/amorphous $Mg_{1.9}M_{0.1}Ni$ alloys were characterized as well.

Keywords: Hydrogen storage materials; Magnesium alloys; Mechanical alloying; Transmission electron microscopy; Thermal analysis; X-ray diffraction

1. Introduction

Mechanical alloying (MA) by high energy ball milling was found to be a promising method for synthesizing novel hydrogen storage materials, including Mg- and Mg_2Ni-based alloys [1–6]. Ball milling (BM) followed by low and intermediate temperature annealing was also successfully applied for producing Mg_2Ni-based nanocrystalline alloys [7,8]. Different alloying elements (e.g., Ti, Zr, V, Al) have been introduced in the nanocrystalline Mg-based materials by controlled BM and improved hydrogen sorption properties were achieved [4,5,9–12]. A synergetic effect of Zr and Ti was found for $Mg_{35}Ti_{10-x}Zr_xNi_{55}$ alloys, which makes the passive film more compact and more protective against corrosion than by Ti and Zr alone [13]. In our recent study [14] the ball milling and heat treatment parameters were optimised with respect to producing amorphous and nanocrystalline (5–20 nm) Mg_2Ni-based alloys from elemental powders. The alloys containing a large amount of amorphous phase after milling, during subsequent annealing form coarser grained nanocrystalline Mg_2Ni (10–20 nm) compared to the alloys prepared by long time milling only (<10 nm). Nanostructured Mg_2Ni-based alloys, prepared by MA as well as by rapid solidification [15], reveal improved hydriding properties, mainly due to the large volume fraction of the grain-boundary regions [16,17].

The present work aims in producing amorphous and nanocrystalline $Mg_{1.9}M_{0.1}Ni$ (M=Ti, Zr, V) alloys with different combinations of the alloying elements by BM and by BM with annealing and studying their hydrogen sorption properties. The microstructure and morphology of the as-milled and annealed after milling powders were characterized as well.

2. Experimental

Pure elemental powders of magnesium, nickel, titanium, zirconium and vanadium were used as starting materials. The ball milling was performed with a laboratory planetary mill (Fritsch P7) with different rotation velocities and ball to powder (B/P) mass ratio 15:1, under argon atmosphere.

*Corresponding author.
E-mail address: tspassov@chem.uni-sofia.bg (T. Spassov).

0925-8388/03/$ – see front matter
doi:10.1016/S0925-8388(03)00122-1

The vials and the balls were made from stainless steel. The samples were handled in a glove box under Ar and the vials were sealed under argon atmosphere. A small amount of the powder was taken from the mill at regular periods of time for structural, morphological and thermal analysis.

The phases and the microstructure were analysed by X-ray diffraction (XRD) using a Philips 3050 diffractometer with Cu Kα radiation and TEM. The diffraction data were analysed by a full pattern fitting procedure (Rietveld method) using the program MAUD [18] and the lattice parameters, the amount of the different phases, the crystallite size and the internal strain were determined. The powder morphology and the chemical composition of the alloys treated under different milling and annealing conditions were studied by scanning electron microscopy with an energy dispersive X-ray analysis (SEM/EDX).

Differential scanning calorimetry analysis, using a Perkin-Elmer DSC-7 calorimeter, was performed in order to study the thermal behavior of the as-milled alloys. Thermal stability of the amorphous and nanocrystalline microstructures obtained by ball milling as well as crystallization of the amorphous alloys were investigated, too.

The P–C-isotherms were measured by using a homemade automatic apparatus (Sievert's type) at 220 °C.

3. Results and discussion

Typical XRD patterns of $Mg_{1.9}M_{0.1}Ni$ (M=Ti, Zr, V) alloys produced by continuous milling at 400 and 480 rpm are shown in Fig. 1. It is seen that after sufficient time of milling the powders reveal nanocrystalline/amorphous microstructure, consisting of mainly hexagonal Mg_2Ni phase. At these concentrations (3 at.%) the alloying elements (Ti, Zr, V) form solid solutions, substituting Mg in the crystal lattice of the Mg_2Ni phase. Influence of the additions on the efficiency of alloying during ball milling

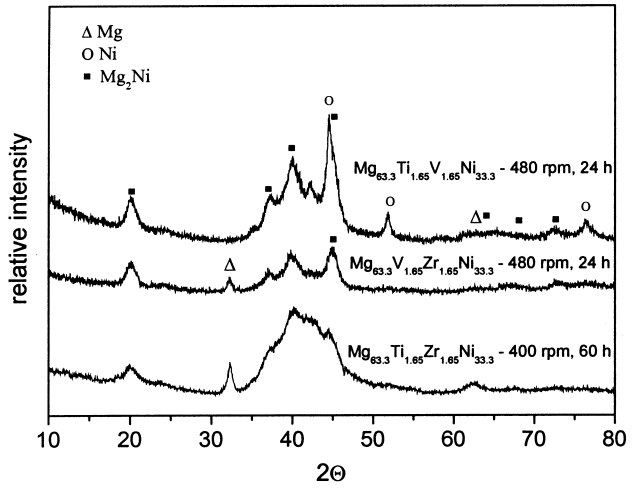

Fig. 1. X-ray diffraction patterns (Cu Kα) of quaternary $Mg_{1.9}M_{0.1}Ni$ (M=Ti, V, Zr) alloys prepared by mechanical alloying.

was not observed. Ball milling causes formation of an amorphous phase, whose amount increases with the time and later crystallizes after continuous milling. The time to reach maximum amorphous fraction depends strongly on the rotation speed as well as on the contamination of the milling atmosphere (Ar). Generally, a larger amount of amorphous phase was obtained at lower rotation velocities. The presence of small amounts of oxygen in the gas phase accelerates the formation of the amorphous phase as well as its further nanocrystallization during milling.

SEM observations reveal that after milling the sample consists of agglomerations (5–50 μm) of smaller particles (1–10 μm) cold welded together [14]. The EDX analysis indicates that Mg and Ni, as well as the alloying elements (Ti, Zr, V) are uniformly distributed in the powder mixture. TEM and electron diffraction of the mechanically alloyed $Mg_{1.9}Ti_{0.05}Zr_{0.05}Ni$ (after 24 h milling at 480 rpm) (Fig. 2) confirm the results from the SEM and XRD analysis. After continuous milling the powder particles (dispersed in acetone) are less than 1 μm and relatively homogeneous in size (Fig. 2a). It can be seen that the particles consist of nanocrystals with average size of about 10–20 nm (Fig. 2b). The size of the nanocrystals determined by TEM is slightly larger than that obtained by XRD (≤10 nm). Selected area diffraction pattern (SADP) from a single particle reveals also that the alloy consists of Mg_2Ni nanocrystals. A small amount of amorphous (disordered) phase can be also detected.

As was already reported [14] BM and subsequent annealing (in the temperature range of 300–400 °C) leads to nanocrystalline Mg_2Ni-based alloys (10–20 nm), too. Crystallization of the ball-milled amorphous powders proceeds during linear heating in the DSC (Fig. 3) at temperatures of about 150 °C and leads to formation of nanocrystalline Mg_2Ni. The second broad exothermic effect, in the temperature range of 180–320 °C, was shown to be due to a solid state interdiffusion reaction between the very fine Mg and Ni particles, brought in close contact during milling [14]. After longer milling times the sample is nearly fully nanocrystallized and subsequent DSC scan reveals only a very small exothermic effect, due to the crystallization of the rest of the amorphous phase, untransformed during the milling process. Fig. 4 shows that milling until amorphization of the powder (12 h at 480 rpm) and then heating up to 400 °C at 10 K/min (curve d) causes almost complete transformation to the Mg_2Ni phase. It was found that the microstructure of the Mg_2Ni-based alloy, crystallized during milling, having an average crystal size of less than 10 nm (curve a), is finer than that of the sample produced by milling until amorphous state and then crystallized by annealing (average crystals size—15 nm, curve d). Fig. 2c shows TEM and selected area diffraction pattern of milled until amorphization (12 h at 480 rpm) and then crystallized by heating up to 400 °C with 10 K/min $Mg_{1.9}Ti_{0.05}Zr_{0.05}Ni$ sample and confirms the XRD results. Generally, varying the milling time and

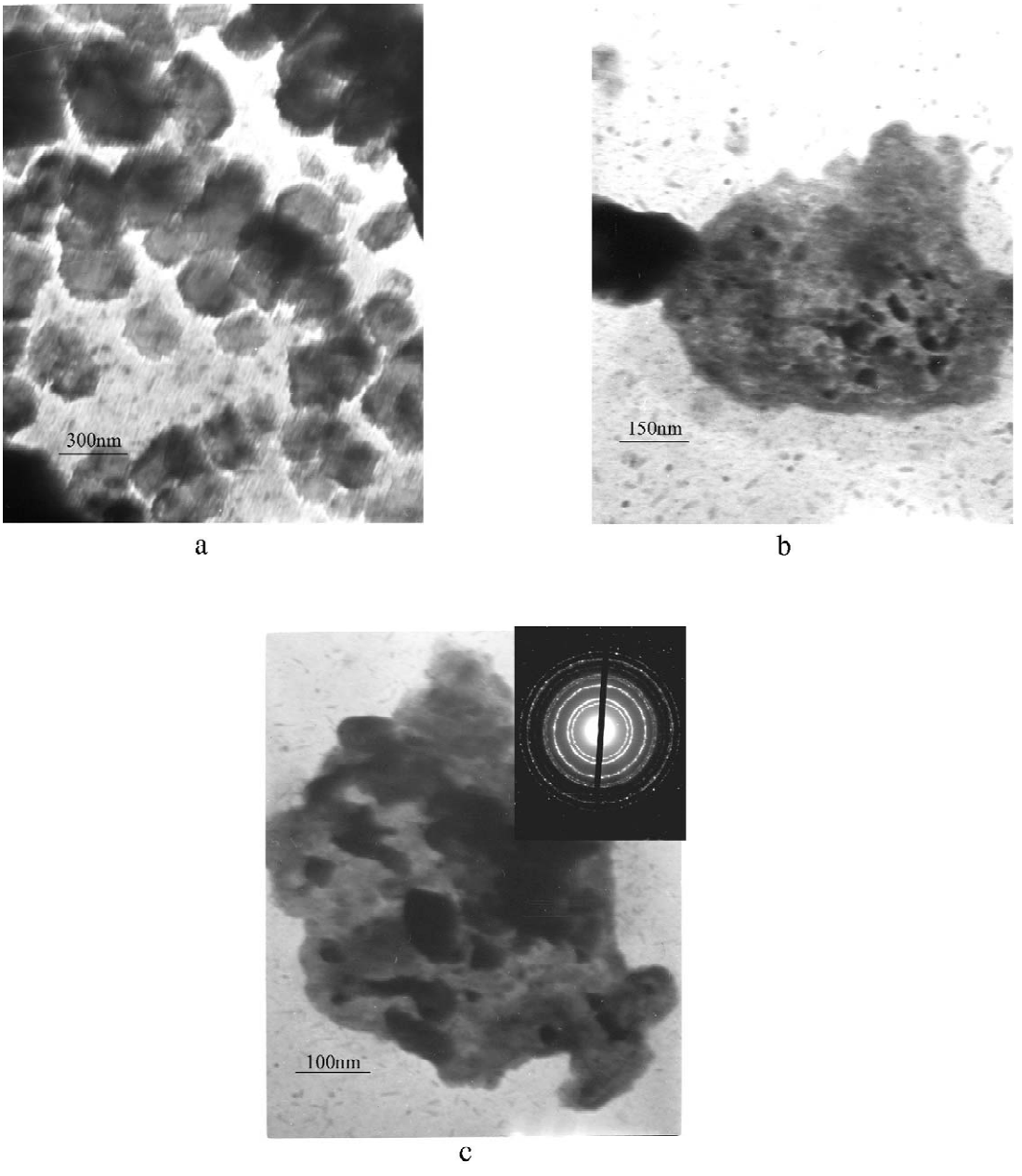

Fig. 2. TEM images and selected area diffraction pattern of mechanically alloyed $Mg_{1.9}(Ti,Zr)_{0.1}Ni$: (a) 24 h at 480 rpm, (b) 24 h at 480 rpm, (c) 12 h at 480 rpm and heating up to 400 °C with 10 K/min.

temperature of annealing (after milling) different microstructures could be obtained (see Figs. 2 and 4).

Preliminary measurements of the hydrogen sorption properties (hydrogen storage capacity and hydrogenation kinetics) for the continuous milled samples were realized, as well. The hydrogen desorption characteristics of the mechanically alloyed $Mg_{1.9}Ti_{0.05}Zr_{0.05}Ni$ (24 h at 480 rpm), containing very small nanocrystals (<10 nm) and amorphous phase, were measured at 220 °C (Fig. 5). The temperature of 220 °C was chosen in order to be high enough for the hydrogen desorption to proceed, but not enough to change essentially the initial microstructure of the alloy even after long time annealing. Fig. 5 shows a kinetic curve of desorption of this alloy at 220 °C under a pressure of 0.1 MPa. For comparison, on the same plot a desorption kinetic curve for a nanocrystalline $Mg_{1.9}Ti_{0.1}Ni$ alloy [11] is also presented, although the desorption conditions are slightly different (250 °C and 0.015 MPa). Both milled alloys, nanocrystalline $Mg_{1.9}Ti_{0.1}Ni$ and nano-/amorphous $Mg_{1.9}Ti_{0.05}Zr_{0.05}Ni$, exhibit a very fast initial desorption rate, much faster than that of the cast Mg_2Ni as well as nanocrystalline Mg_2Ni [11]. More than 65% of the hydrogen is desorbed within about 10 min. The enhanced desorption kinetics of the Ti and Zr substituted alloys, compared to Mg_2Ni, are mainly due to the very fine nanocrystalline/amorphous microstructure of the mechani-

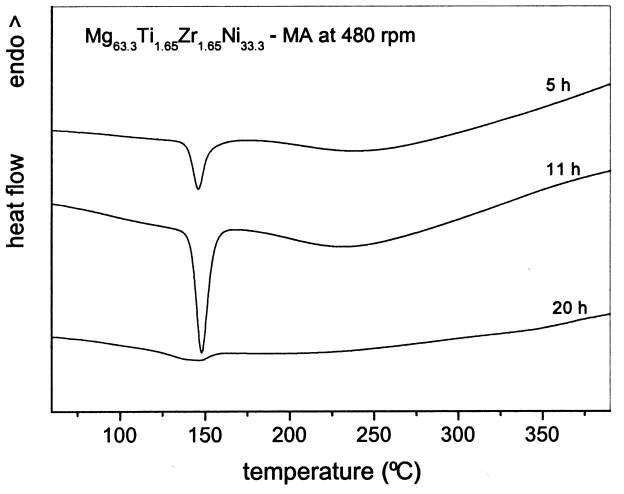

Fig. 3. DSC scans of $Mg_{1.9}(Ti,Zr)_{0.1}Ni$ alloys after different times of milling at 480 rpm.

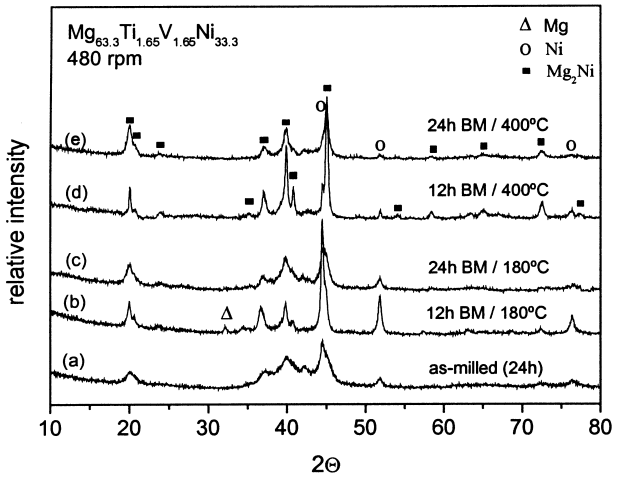

Fig. 4. XRD patterns of ball-milled $Mg_{1.9}(Ti,Vr)_{0.1}Ni$ alloy (480 rpm) after different milling and heat treatments (by DSC with 10 K/min).

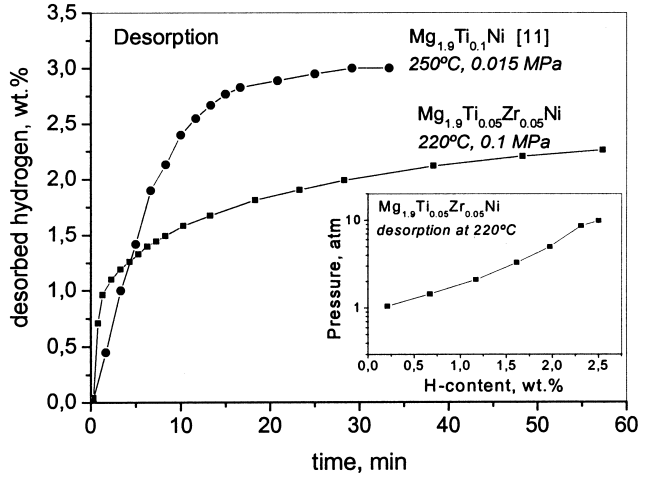

Fig. 5. Hydrogen desorption isotherms and pressure–composition–temperature diagram (inset) of mechanically alloyed nano-/amorphous $Mg_{1.9}(Zr,Ti)_{0.1}Ni$ (24 h at 480 rpm) at 220 °C.

cally alloyed powder materials. The increased volume of the unit cell with Zr is also beneficial for hydrogen diffusion in the alloy. The lower hydrogen capacity of $Mg_{1.9}Ti_{0.05}Zr_{0.05}Ni$ (2.3 wt.%) compared to the $Mg_{1.9}Ti_{0.1}Ni$ [11] (about 3 wt.%) is due to the finer nanocrystals (<10 nm) and the presence of amorphous (disordered) phase in the material synthesised by us.

The P–C isotherms of the $Mg_{1.9}M_{0.1}Ni$ alloys with different alloying elements (M=Ti, Zr, V) do not differ essentially and are typical for amorphous or very fine nanocrystalline-amorphous materials (Fig. 5, inset). The isotherms do not contain a clear plateau, which is in agreement with the nano-/amorphous microstructure of the alloys after prolonged milling (24 h at 480 rpm), proved by XRD. The maximum hydrogen content is about 2.3 wt.% under a hydrogen pressure of 1 MPa at 220 °C. It was recently shown [19] that the hydrogen desorption temperature of mechanically alloyed nanocrystalline/amorphous Mg_2Ni is lowered by about 90 °C (from 300 to 210 °C), whereas the hydrogen capacity is decreased by about 1.4 wt.% (from 3.6 to 2.25 wt.%) as compared to the hydrogen storage capacity of polycrystalline Mg_2Ni [20], which is in agreement with the results of the present study. The maximum hydrogen content, 2.0–2.3 wt.%, obtained for nano-/amorphous Mg_2Ni-based alloys produced by MA (present study) and by melt-spinning [15] is in very good agreement with the values determined by Orimo and Fujii [17] for nanostructured Mg–Ni alloys, composed of Mg_2Ni nanograins (~10 nm) and amorphous MgNi regions, dispersed around the nanocrystals. Although it is not possible to determine a plateau pressure of hydrogen (due to the continuous slope of the P–C isotherm) (Fig. 5, inset), it is seen that generally the substitution of Mg by Ti and Zr in Mg_2Ni destabilizes the Mg_2Ni-based hydride compared to the nanocrystalline Mg_2Ni [11].

A comprehensive study on the hydrogen sorption properties of Mg_2Ni-based alloys with different alloying additions and in a different microstructural state (amorphous, nano-/amorphous, nanocrystalline) is underway.

4. Conclusions

Amorphous and nanocrystalline $Mg_{1.9}M_{0.1}Ni$ (M=Ti, Zr, V) alloys were produced by ball milling and by milling with subsequent annealing. Depending on the milling (rotation speed and time of milling) and annealing (temperature and time of annealing) conditions different microstructures were obtained. The time to reach almost full amorphization by ball milling at different rotation velocities was determined. Continuous milling leads to nanocrystallization of the amorphous phase. By short time annealing at medium temperatures (300–400 °C) the ball-milled amorphous samples transforms to nanocrystalline state too, as the size of the nanocrystals are larger (10–20 nm) than that created only by milling (5–10 nm).

Preliminary hydrogen absorption/desorption study shows that the nano-/amorphous $Mg_{1.9}M_{0.1}Ni$ (M=Ti, Zr, V) alloys produced by continuous milling reveal improved H-sorption kinetics compared to the nanocrystalline Mg_2Ni. In order to achieve higher hydrogen capacity a controlled increase of the nanocrystals size has to be realized by crystallization and grain growth of the nano-/amorphous ball-milled alloys.

Acknowledgements

One of the authors (T.S.) is very grateful to the Ministry of Education, Culture and Sports of Spain for the financial support. The work has been also supported by the project 2001-SGR-00189 and EU RTN2-2001-00176.

References

[1] L. Zaluski, A. Zaluska, J.O. Ström-Olsen, J. Alloys Comp. 253–254 (1997) 70.
[2] S. Ruggeri, C. Lenain, L. Roue, H. Alamdari, G. Liang, J. Huot, R. Schulz, Mater. Sci. Forum 37 (2001) 63–70.
[3] L. Guanglie, C. Linshen, W. Lianbang, Y. Huantang, J. Alloys Comp. 321 (2001) L1–L4.
[4] T.W. Hong, Y.J. Kim, J. Alloys Comp. 330–332 (2002) 584–589.
[5] H.Y. Lee, N.H. Goo, W.T. Jeong, K.S. Lee, J. Alloys Comp. 313 (2000) 258–262.
[6] S.S. Sai Raman, D.J. Davidson, J.-L. Bobet, O.N. Srivastava, J. Alloys Comp. 333 (2002) 282–290.
[7] L. Aymard, M. Ichitsubo, K. Uchida, E. Sekreta, F. Ikazaki, J. Alloys Comp. 259 (1997) L5–L8.
[8] Y. Zhang, H. Yang, H. Yuan, E. Yang, Z. Zhou, D. Song, J. Alloys Comp. 269 (1998) 278–283.
[9] S. Nohara, K. Hamasaki, S. Guo Zhang, H. Inoue, C. Iwakura, J. Alloys Comp. 280 (1998) 104–106.
[10] S.C. Han, P.S. Lee, J.Y. Lee, A. Züttel, L. Schlapbach, J. Alloys Comp. 306 (2000) 219–226.
[11] G. Liang, J. Huot, S. Boily, A. Van Neste, R. Schulz, J. Alloys Comp. 282 (1999) 286–290.
[12] Y. Zhang, B. Liao, L.X. Chen, Y.Q. Lei, Q.D. Wang, J. Alloys Comp. 327 (2001) 195–200.
[13] Y. Zhang, Y. Lei, L. Chen, J. Yuan, Z. Zhang, Q. Wang, J. Alloys Comp. 337 (2002) 296–302.
[14] T. Spassov, P. Solsona, S. Suriñach, M.D. Baró, J. Alloys Comp. 349 (2003) 242–254.
[15] T. Spassov, U. Köster, J. Alloys Comp. 279 (1998) 279.
[16] K. Lu, R. Lück, B. Predel, Acta Metall. Mater. 42 (1994) 2303.
[17] S. Orimo, H. Fujii, Appl. Phys. A 72 (2001) 167–186.
[18] L. Lutterotti, S. Giolanella, Acta Mater. 46 (1997) 101.
[19] T.W. Hong, S.K. Kim, Y.J. Kim, J. Alloys Comp. 312 (2000) 60–67.
[20] J.J. Reilly, R.H. Wiswall, Inorg. Chem. 7 (1968) 2254.